Theses and Dissertations | 1. Thesis and Dissertation Collection, all items

1997-06

Acoustic Casimir effect

Holmes, Christopher David

Monterey, California. Naval Postgraduate School

http://hdl.handle.net/10945/7844

NAVAL POSTGRADUATE SCHOOL
Monterey, California

THESIS

ACOUSTIC CASIMIR EFFECT

by

Christopher David Holmes

June, 1997

Thesis Advisor:	Andrés Larraza
Co-Advisor:	Bruce C. Denardo

REPORT DOCUMENTATION PAGE

Form Approved OMB No. 0704-0188

1. AGENCY USE ONLY (Leave blank)	2. REPORT DATE June 1997	3. REPORT TYPE AND DATES COVERED Master's Thesis

4. TITLE AND SUBTITLE	5. FUNDING NUMBERS
A COUSTIC CASIMIR EFFECT	

6. AUTHOR(S)

Holmes, Christopher D.

7. PERFORMING ORGANIZATION NAME(S) AND ADDRESS(ES) Naval Postgraduate School Monterey CA 93943-5000	8. PERFORMING ORGANIZATION REPORT NUMBER
9. SPONSORING/MONITORING AGENCY NAME(S) AND ADDRESS(ES)	10. SPONSORING/MONITORING AGENCY REPORT NUMBER

11. SUPPLEMENTARY NOTES The views expressed in this thesis are those of the author and do not reflect the official policy or position of the Department of Defense or the U.S. Government.

12a. DISTRIBUTION/AVAILABILITY STATEMENT Approved for public release; distribution is unlimited.	12b. DISTRIBUTION CODE

13. ABSTRACT (maximum 200 words)

In 1948, Hendrick Brugt Gerhard Casimir predicted that two closely spaced uncharged conducting plates in vacuum would be mutually attracted. This attractive force is an indirect manifestation of the quantum electromagnetic zero point field (ZPF). When the indirect manifestations of the ZPF are interpreted as due to radiation pressure, acoustic noise can provide an excellent analog to investigate the Casimir effect as well as other effects due to the ZPF. Force measurements between two parallel plates are performed in an acoustic chamber with a broadband noise spectrum within a 5-15 kHz band and an intensity of 133 dB (re 20 μPa). When the results are compared with the appropriate theory, very good agreement is obtained. Applications of the acoustic Casimir effect to noise transduction can provide new means to measure background noise. Because attractive or repulsive forces can be obtained by adjusting the noise spectrum or the plate geometry, a non-resonant method of acoustic levitation is also suggested.

14. SUBJECT TERMS: Casimir Effect - Analog to Zero Point Field (ZPF)			15. NUMBER OF PAGES 45
			16. PRICE CODE

17. SECURITY CLASSIFI-CATION OF REPORT Unclassified	18. SECURITY CLASSIFI-CATION OF THIS PAGE Unclassified	19. SECURITY CLASSIFI-CATION OF ABSTRACT Unclassified	20. LIMITATION OF ABSTRACT UL

NSN 7540-01-280-5500

Standard Form 298 (Rev. 2-89)
Prescribed by ANSI Std. 239-18 298-102

ACOUSTIC CASIMIR EFFECT

Christopher D. Holmes
Lieutenant, United States Navy
B.S., Cornell University, 1988

Submitted in partial fulfillment
of the requirements for the degree of

MASTER OF SCIENCE IN
APPLIED PHYSICS
from the

NAVAL POSTGRADUATE SCHOOL
June 1997

ABSTRACT

In 1948, Hendrick Brugt Gerhard Casimir predicted that two closely spaced uncharged conducting plates in vacuum would be mutually attracted. This attractive force is an indirect manifestation of the quantum electromagnetic zero point field (ZPF). When the indirect manifestations of the ZPF are interpreted as due to radiation pressure, acoustic noise can provide an excellent analog to investigate the Casimir effect as well as other effects due to the ZPF. Force measurements between two parallel plates are performed in an acoustic chamber with a broadband noise spectrum within a 5-15 kHz band and an intensity of 133 dB (re 20 μPa). When the results are compared with the appropriate theory, very good agreement is obtained. Applications of the acoustic Casimir effect to noise transduction can provide new means to measure background noise. Because attractive or repulsive forces can be obtained by adjusting the noise spectrum or the plate geometry, a non-resonant method of acoustic levitation is also suggested.

TABLE OF CONTENTS

viii

ACKNOWLEDGEMENT

I. INTRODUCTION

In 1948, the Dutch physicist, Hendrik Brugt Gerhard Casimir made the quantum electromagnetic prediction that two closely spaced uncharged conducting plates would be mutually attractive (Casimir, 1948). Due to the presence of the plates, the mode structure of the quantum electromagnetic zero point field (ZPF) changes relative to free space. The difference between the vacuum electromagnetic energy for infinite plate separation and a finite plate separation is the interaction energy between the plates, from which the force is calculated. If the plates are a distance d apart, the force per unit area is proportional to $\hbar c/d^4$. Although this result can be proven rigorously, it can be easily shown by dimensional analysis that this is the only possible combination in which $\hbar$, c, and d can be united to yield a force per unit area. The constant of proportionality is a pure number, and a rigorous calculation yields the value $\pi^2/240$.

This force, although small, is larger than the gravitational force for separation distances smaller than

$$\sqrt[4]{\frac{\pi\hbar c}{480 G\sigma^2}} \,, \qquad\qquad (1.1)$$

where σ is the surface mass density. For 0.5 μm thick silver plates the distance in Eq. (1.2) is 700 μm. An order of magnitude smaller distance would yield a Casimir force that is four orders of magnitude bigger than the gravitational force.

Physically, the electromagnetic ZPF fluctuations induce local dipoles in both plates and because of the spatial correlations of the fluctuations the interaction of these dipoles leads to a net attractive force. Based on this argument, there must also be a Casimir force between two parallel dielectric plates (Lifshitz, 1956 and Schwinger et al., 1978).

The attraction between the two parallel plates can also be understood superficially in terms of the radiation pressure exerted by the plane waves that comprise the homogeneous, isotropic ZPF spectrum. In the space between the conducting plates, the modes formed by reflections off the plates act to push the plates apart. The modes outside the cavity formed by the plates act to push the plates together. The total outward pressure and the total inward pressure are infinite, but it is only the difference that is physically meaningful. This difference leads to an attractive force.

As shown by Fig. 1.1, recent interest in the Casimir effect has grown significantly since databasing in 1961. The graph in Fig 1.1 when viewed as social phenomenon in science, may indicate that similar to early quantum mechanics at the turn of this century, zero-point field effects may become a new paradigm in physics at the turn of the next century.

Source: Science Citation Index (1961-1996)
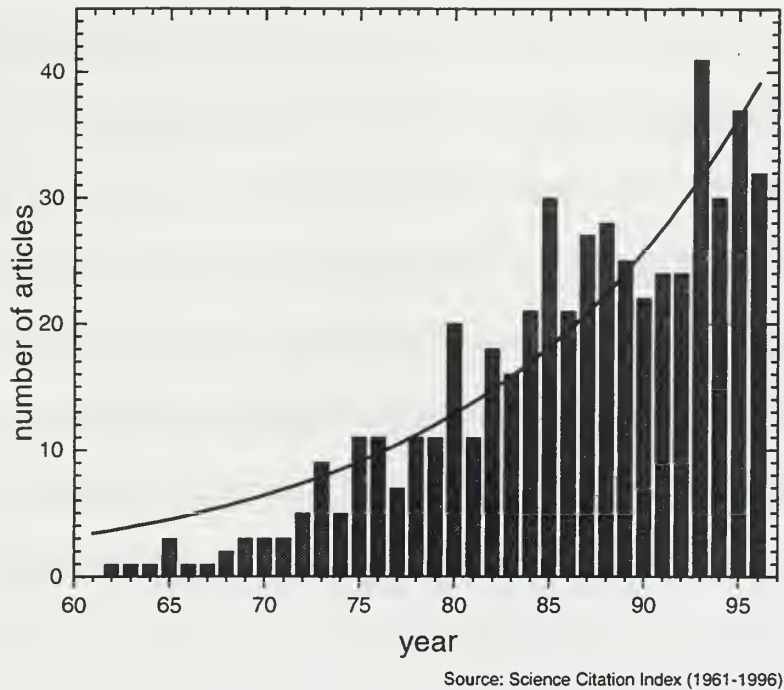
Figure 1.1. The growth of interest in the Casimir effect is reflected by the direct reference to Casimir's original 1948 published work entitled "On the attraction between two perfectly conducting plates" (Casimir, 1948). As a reference, the data has been fitted to an exponential.

The ZPF is homogeneous and isotropic (the same at all points of space and time, and in all directions). It is also Lorentz invariant (any two inertial observers do not see a difference). One can say that the ZPF is undetectable in any inertial frame because homogeneity, isotropy, and Lorentz invariance do not allow an observer to see any contrast between directions, times, and inertial frames. The Casimir effect is one of the several indirect manifestations of the ZPF. Other indirect manifestations include the van der Waals force between polarizable matter (Casimir and Polder, 1948), spontaneous emission of radiation, and the Lamb shift (Sakurai, 1967).

3

Recently, two new results have been obtained from the properties of the ZPF. In the first of these results, Schwinger (1993) and Eberlein (1996), in an attempt to explain the emission of light from a collapsing bubble (sonoluminescence), have predicted that the accelerated walls of a dielectric cavity emit nondipolar broadband light due to nonadiabatic changes of the volume. Physically, because the electromagnetic ZPF excites fluctuating dipoles on the stationary surface of a dielectric discontinuity (a mirror), virtual two-photon states are perpetually excited by the mirror in the vacuum. However, the fluctuating forces on either side of the mirror are balanced against each other, so that no mean radiation pressure acts on the mirror. Because of Lorentz invariance, a mirror moving with constant velocity would not experience any mean radiation pressure either. However, when the mirror accelerates the fluctuating dipoles become a source of radiation. For sonoluminescent bubbles, the peak acceleration at the minimum radius is calculated to be about 13 tera g's with a turnaround time of 10 ps. Even if this "Casimir radiation" mechanism does not adequately explain sonoluminescence, it should be tested experimentally.

In the second recent result using the properties of the ZPF, Haisch, Rueda, and Puthoff (1994) have put forward the proposal that inertia, and hence Newton's second law, can be *derived* from first principles in terms of the ZPF. Because gravitational mass and inertial mass are equivalent, this idea would make gravitation an electromagnetic effect.

A Lorentz transformation Doppler shifts the frequency and also alters the intensity of radiation. The only spectral shape that is the same for any inertial

frame is proportional to the cube of the frequency (Boyer, 1969). This spectral

shape implies an energy per mode proportional to the frequency in agreement

with the quantum zero-point energy $\frac{1}{2}\hbar\omega$ per mode of the electromagnetic

vacuum.

At finite temperatures, there must also be a force between the plates due

to the real photons. Thus, the Casimir effect is the zero-temperature limit of the

electromagnetic radiation pressure. However, thermal effects can be ignored

when $\hbar\omega \gg k_B T$, where k_B is Boltzmann constant. The lowest frequency that

contributes to the radiation pressure inside the plates is $\omega = \pi c/d$. Thus thermal

effects can be ignored for separations $d < \pi\hbar c / k_B T$. At room temperature this

corresponds to a distance of about 50 μm.

If the ZPF can be thought of as broadband noise of an infinite spectrum, it

should be possible to use an acoustic broadband noise spectrum as an analog

to the ZPF. An acoustic spectrum has several advantages. Because the speed

of sound is six orders of magnitude less than the speed of light, length and time

scales are more manageable and measurable. Also, in an acoustic field, the

shape of the spectrum as well as the field intensity can be controlled.

We refer to this new area of research as *Casimir acoustics*. By analogy

to the Casimir effect, the measurement of the force between two plates in a

homogeneous, isotropic, acoustic field is the acoustic Casimir effect. Also,

Casimir acoustics may provide a powerful tool in the testing of recently proposed

ZPF effects such as the broadband acoustic radiation emitted by a cavity whose

walls are made to oscillate at a high frequency (predicted Casimir radiation), the

5

change in the frequency of oscillation of a pendulum as the noise intensity is varied (suggested origin of inertia), and the force of attraction between two spheres due to acoustic shadowing (van der Waals force and suggested origin of gravitation).

The purpose of this thesis is to measure the force between two parallel plates in a homogeneous, isotropic acoustic noise filed. The noise spectrum is nearly flat and in a band of frequencies. In Chapter II we derive the force law for such an spectrum. In Chapter III, we give details of the apparatus. Chapter IV presents the results of the measurements and compares them with theory, and provides conclusions and possible applications.

II. THEORY

One of the key ideas in the derivation of the ZPF Casimir force is the fact that the energy per mode $\frac{1}{2}\hbar\omega$ remains the same. Thus, the space between the plates cannot be considered as a resonant cavity. That this is true, can be understood by using the adiabatic theorem. To this purpose, imagine that the plates are initially far apart so that the spectrum of the ZPF is that of free space $\hbar\omega^3/2\pi^2c^3$. If we now adiabatically move the walls towards each other, the modes comprising the ZPF will remain in their ground state; only their frequencies will be shifted in such a way that the ratio of the energy per mode E to the frequency ω remains constant, or

$$\frac{E}{\omega} = \frac{1}{2}\hbar \,. \tag{2.1}$$

Thus, the main effect of the boundaries is to redistribute ground state modes of which there is an infinite number.

In contrast to the ZPF Casimir effect, in the acoustic Casimir effect the adiabatic theorem does not apply both because of inherent losses in the system and because the spectrum can be made arbitrary. Also, while external drivers can provide a steady state noise spectrum from which we can infer the energy per mode by dividing by the density of states ω^2/π^2c^3, this value may change in the cavity formed by the plates because of Q amplification. However, for this

resonant cavity configuration Q is very small and we may assume it to be equal to unity, rendering the energy per mode equal to its value in free space.

The acoustic shape of the spectrum is determined mainly by the frequency response of the drivers. Good acoustic drivers have a flat response over a frequency band. With appropriate filters, one may shape the spectrum within the driver's frequency response and obtain, in principle different force laws. We specialize the derivation of the force law below for a flat spectral shape over a finite frequency band.

The radiation pressure of a wave incident at angle θ on a rigid plate is

$$P = \frac{2I}{c} \cos^2(\theta) , \qquad (2.2)$$

where I is the average intensity of the incident wave and c is the wave speed. The factor of two is due to perfect reflectivity assumed for the plate. We consider broadband acoustic noise of *constant* spectral intensity I_ω in a band of frequencies from ω_1 to ω_2. The corresponding spectral intensity in the wavevector space of traveling waves is

$$I_k = \frac{cI_\omega}{4\pi k^2} , \qquad (2.3)$$

where the wavevector is $\mathbf{k} = (k_x, k_y, k_z)$ whose magnitude is the wavenumber $k=\omega/c$. We choose the z axis to be normal to the plate, so that $k_z = k\cos(\theta)$. From Eq. (2.2), the total radiation pressure due to waves that strike the plate is

then

$$P = \frac{2}{c} \int dk_x dk_y dk_z I_k \cos^2(\theta) = \frac{I_\omega}{2\pi} \int dk_x dk_y dk_z \frac{k_z^2}{k^4} \, , \tag{2.4}$$

where the integration is over **k** values corresponding to waves that strike the plate. Converting Eq. (2.4) to polar coordinates, and performing the azimuthal integration, yields

$$P = I_\omega \int_{\theta=0}^{\pi/2} d\theta \sin(\theta) \cos^2(\theta) \int_{k=k_1}^{k_2} dk \, . \tag{2.5}$$

Performing the integrations in Eq. (2.5) yields $P = I_\omega(k_2 - k_1)/3$, which can be expressed simply as

$$P = \frac{I}{3c} \, , \tag{2.6}$$

where the total intensity of the noise is $I = I_\omega(\omega_2 - \omega_1)$. Although Eq. (2.6) was derived for a constant spectral density I_ω, it can readily be shown to be valid for *any* isotropic spectral distribution. Eq. (2.6) can be understood by a simplistic approach: If one-sixth of the intensity is considered to be propagating in each of six possible orthogonal directions, then the radiation pressure (2.2) becomes $2(I/6c)$, which is identical to Eq. (2.6).

Broadband noise outside two parallel rigid plates drives the discrete modes between the plates. For convenience, we continue to deal with the

traveling wave (rather than standing wave) modes, which we label with wavevector components $k_x = n_x\pi/L_x$, $k_y = n_y\pi/L_y$, and $k_z = n_z\pi/L_z$, where n_x, n_y, and n_z are signed integers and L_x, L_y, and L_z are the dimensions between the plates. As in the previous analysis, the z axis is chosen to be normal to the plates. As a result of the quality factor of the modes being approximately unity, the intensity $I_{in}(\mathbf{k})$ of each mode between the plates is expected to be approximately the same as the outside broadband intensity in a bandwidth equal to the wavevector spacing of the inside modes: $I_{in}(\mathbf{k}) = I_k \Delta k_x \Delta k_y \Delta k_z$, where I_k is given by Eq. (2.3) and where $\Delta k_i = \pi/L_i$. In the limit of large dimensions, the inside intensity gives rise to the correct wavevector spectral intensity I_k. From Eq. (2.2), the pressure on a plate due to the inside modes is

$$P_{in} = \frac{2}{c}\sum I_{in}(\mathbf{k})\frac{k_z^2}{k^2}, \qquad (2.7)$$

where the sum is over values of $\mathbf{k}$ corresponding to modes that strike the plate, which we can take to be those for which $n_z > 0$. We assume that the dimensions L_x and L_y of the plates are sufficiently large, that the corresponding wavevectors are essentially continuous. In comparison to Eq. (2.4), the total inside pressure (2.2) is therefore

$$P_{in} = \frac{I_\omega}{2\pi}\sum \Delta k_z \int dk_x dk_y \frac{k_z^2}{k^4}. \qquad (2.8)$$

We now let $n = n_z$ and $d = L_z$, and define the fundamental transverse

wavenumber (perpendicular to the plates) to be $k_o = \pi/d$.   As in Eq. (2.5) the range of values of k is in a spherical shell of thickness $(k_2 - k_1)$. However, it is easier to calculate the radiation pressure (2.8) in this shell by performing an integration over a sphere of radius k_2 and subtracting the integration over a sphere of radius k_1. Employing polar coordinates for the parallel wavevector, and performing the azimuthal integration, yields

$$P_{in} = k_o^3 I_\omega \sum_{n=1}^{[k_2/k_0]} n^2 \int_0^{\sqrt{k_2^2 - k_o^2 n^2}} \frac{\kappa d\kappa}{\left(\kappa^2 + k_o^2 n^2\right)^2} - (k_2 \rightarrow k_1) \ , \qquad (2.9)$$

where [u] stands for the greatest integer not larger than u. Transforming to the dimensionless variable $x = (\kappa/k_o)^2$ leads to

$$P_{in} = \frac{\pi I_\omega}{2d} \sum_{n=1}^{[k_2 d/\pi]} n^2 \int_0^{(k_2 d/\pi)^2 - n^2} \frac{dx}{\left(x + n^2\right)^2} - (k_2 \rightarrow k_1) \ . \qquad (2.10)$$

The difference $P_{in} - P_{out}$ is the force f per unit area between the plates. Performing the integrals and sums we obtain

$$f = \frac{\pi I_\omega}{2d} \left(N_2 - N_1 - \frac{N_2 (N_2 + 1)(2N_2 + 1)}{6(k_2 d/\pi)^2} + \frac{N_1 (N_1 + 1)(2N_1 + 1)}{6(k_1 d/\pi)^2} - \frac{2(k_2 - k_1)d}{3\pi} \right) \ (2.11)$$

where $N_{1,2} = [k_{1,2} d/\pi]$.

Eq (2.11) is continuous and piecewise differentiable and it can alternate between negative (attractive force) and positive (repulsive force) values. On the other hand, if the lower frequency in the band is zero, the force is always attractive. Figures 2.1 and 2.2 are plots of the negative of Eq. (2.10) for the frequency bands between 5 – 15 kHz and 7.5 – 15 kHz, respectively. The noise intensity in both cases is 133 dB. The plate diameter is set to be 15 cm.

Figure 2.1. Plot of the force between two parallel rigid plates, 15 cm in diameter, as a function of the separation between them, from Eq. (2.11). The force is due to the radiation pressure of flat noise between 5 kHz -15 kHz. The total intensity of the noise is 133 dB (re 10^{-12} W/m^2).
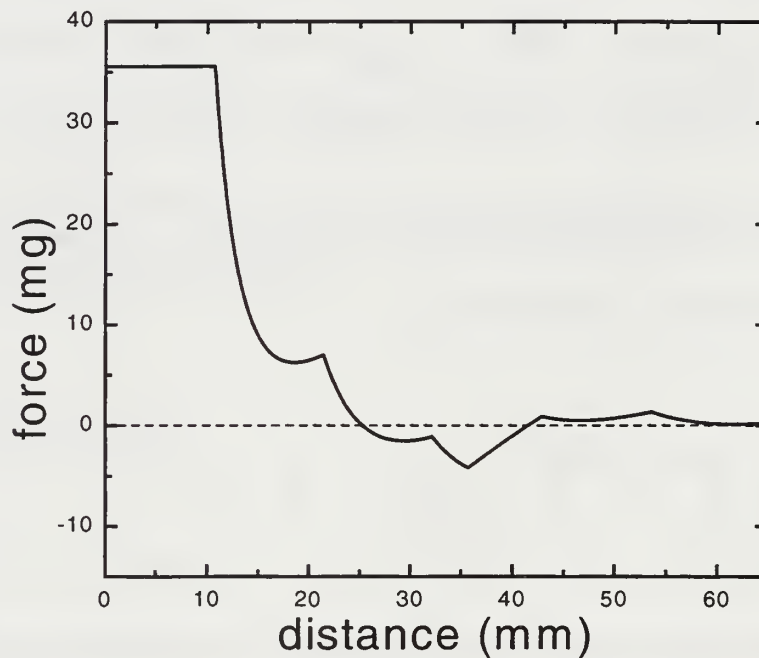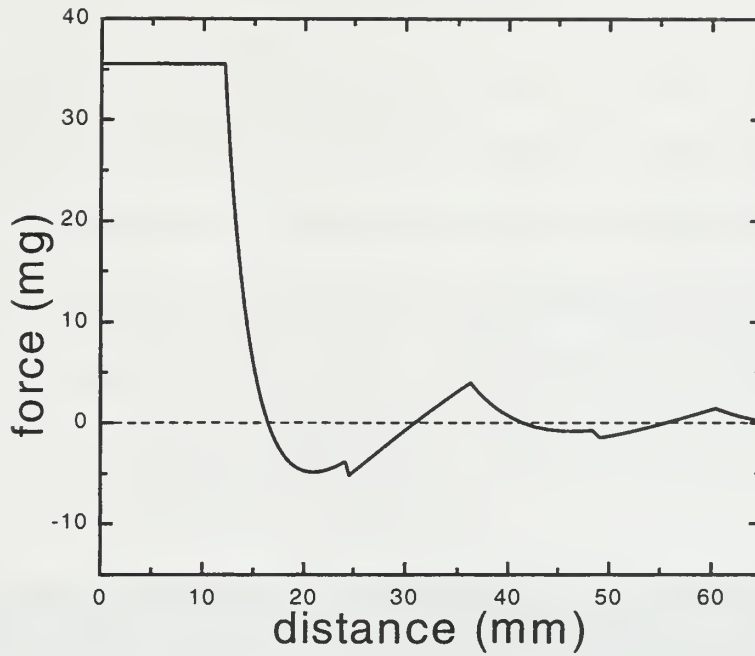
Figure 2.2. Plot of the force between two parallel rigid plates, 15 cm in diameter, as a function of the separation between them, Eq (2.11). The force is due to the radiation pressure of flat noise between 7.5 kHz -15 kHz. The total intensity of the noise is 133 dB (re 10^{-12} W/m^2).

Note that as the lower frequency of the band decreases, the distance at which the force becomes repulsive increases. For the case when the spectrum extends over an infinite interval $(0,\infty)$ the force reduces to the value

$$f = -\frac{\pi I_\omega}{4d} \; ,$$

(2.12)

corresponding to an attractive force.

III. APPARATUS

The equipment for the acoustic Casimir effect experiment, Figure 3.1, consists of three major components: acoustic chamber, optical bench with step motor, and analytical balance. The acoustic chamber provides a nearly homogeneous, isotropic sound field. The internal optical bench with step motor provides precise plate separation, and the analytical balance provides the force measurement for the acoustic Casimir effect. The instrumentation and equipment orientation are outlined in Figure 3.2.
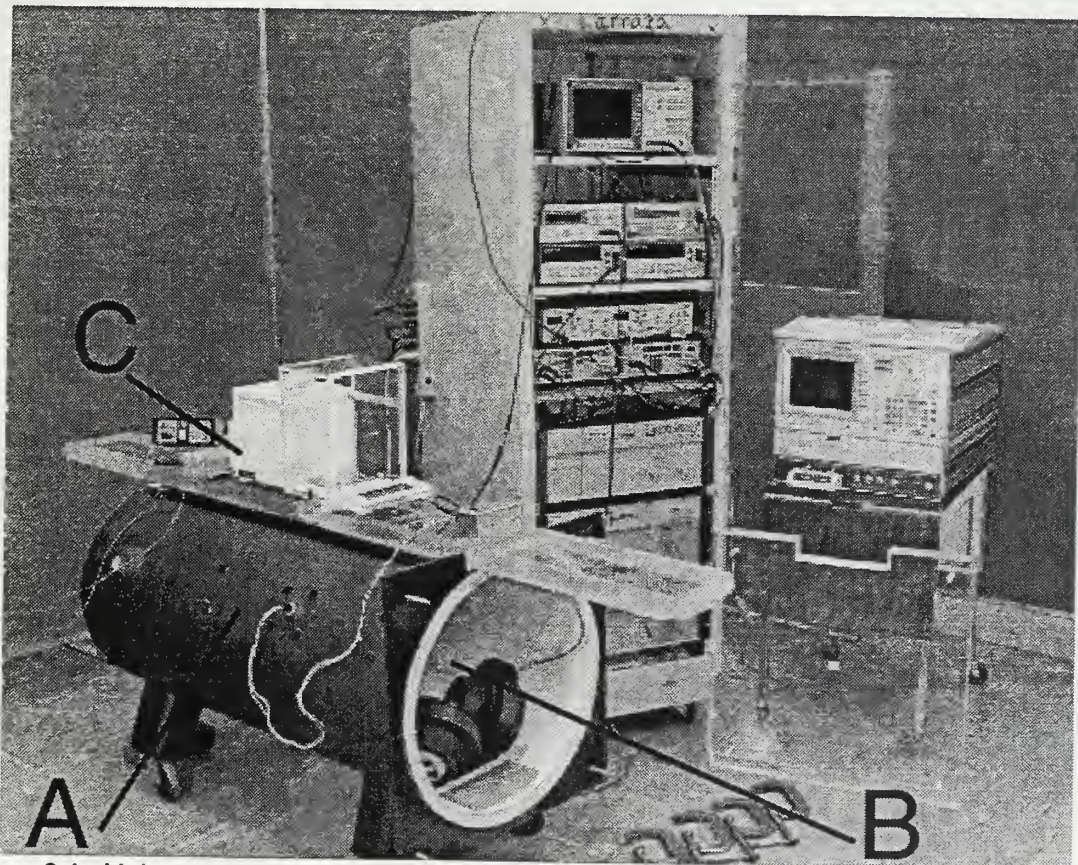
Figure 3.1. Major components of acoustic Casimir experiment. **A.** Acoustic chamber, which provides homogeneous, isotropic acoustic field. **B.** Internal optical bench with step motor, which provides precise plate separation. **C.** Analytical balance mounted on top, which provides the force measurement (below-balance weighing).
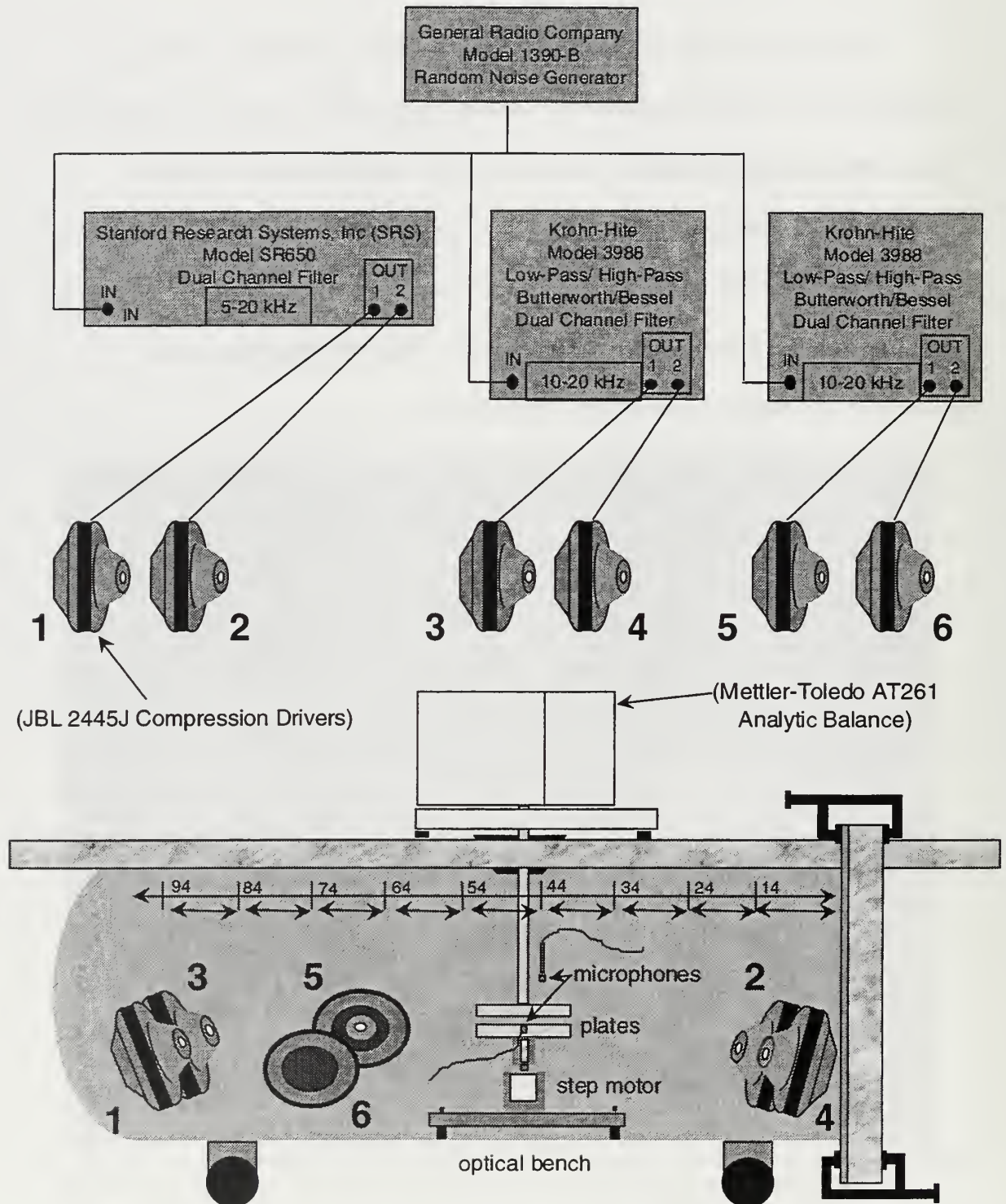
Acoustic Chamber Instrumentation

Figure 3.2. Acoustic chamber instrumentation and compression driver locations.

A.   ACOUSTIC CHAMBER

1.   Tank

The acoustic chamber (Susbilla, 1996) is a converted cylindrical air compressor tank mounted on wheels for mobility. The tank is made of 1/4 inch (0.635 cm) steel, 1.5 m long and 0.5 m in diameter covered with 0.07 inch (1.78 mm) automotive sound deadening self-adhesive pads. The addition of the pads lowered the quality factor (Q) of flexural modes of the cylinder and increased the acoustic impedance of the cylinder walls thereby minimizing transmission losses. The drivers in the acoustic chamber are capable of providing an acoustic noise field of intensity as large as 130 dB (re 20 μPa). One end of the cylinder is ellipsoidal while the other is flat with a steel faceplate that mounts a 4.85 cm (2 in.) thick, 61.5 cm square plexiglass access cover secured by four C-clamps. There is a rubber gasket on the faceplate to improve the seal with the square plexiglass.

2.   Compression Drivers

Six JBL 2445J compression drivers provide the desired acoustic noise intensity within the acoustic chamber. The voltage source for the compression drivers is a General Radio Company 1390-B random noise generator. The random noise generator output is passed through three bandpass filters each followed by dual channel amplifiers, Figure 3.2. One filter is a 115 dB/octave bandpass filter (SRS SR650) set at a band of 5 to 15 kHz. The other two filters

are 48 dB/octave band pass filters (Krohn-Hite 3988) set at a band of 10 to 15 kHz. The separate bandpass filters allowed the flexibility of manipulating the spectral shape of the noise. The filter outputs are amplified by three dual channel Techron 5530 power amplifiers.

3. Spectrum

Acoustic field measurements were made within the tank, Figure 3.3, using a sensing probe with a mounted Larson Davis ¼ inch microphone that has a flat response (±1 dB up to about 22 kHz and ±2 dB to 90 kHz). Measurements were taken at high, center, low, left and right positions along the length of the tank (14-94 cm), and showed the that the six compression drivers were capable of providing a homogeneous isotropic field between 5 and 20 kHz.

Figure 3.3. Sensing design for acoustic chamber that provides homogeneous, isotropic verification measurements. The metallic sphere provides azimuthal motion while the bar gives vertical motion. The noise distribution inside the chamber was probed and the three dimensional isotropy of the noise tested. A Larson Davis ¼" microphone is mounted at bottom of probe.
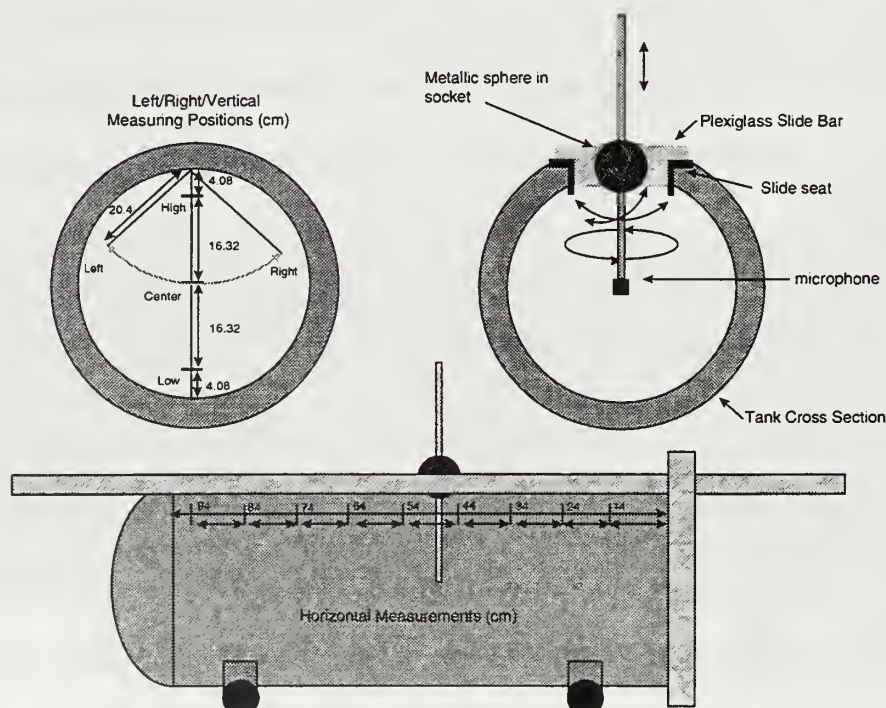
18

Figure 3.4 is a plot of the acoustic field intensity measurements for three horizontal positions (left-right 33-44-54 cm) and three vertical positions (high-low-center), covering the internal location of the optical bench with step motor. The spectrum is essentially flat from 5 kHz to 15 kHz, and rolls off 20 dB from 15 to 20 kHz.
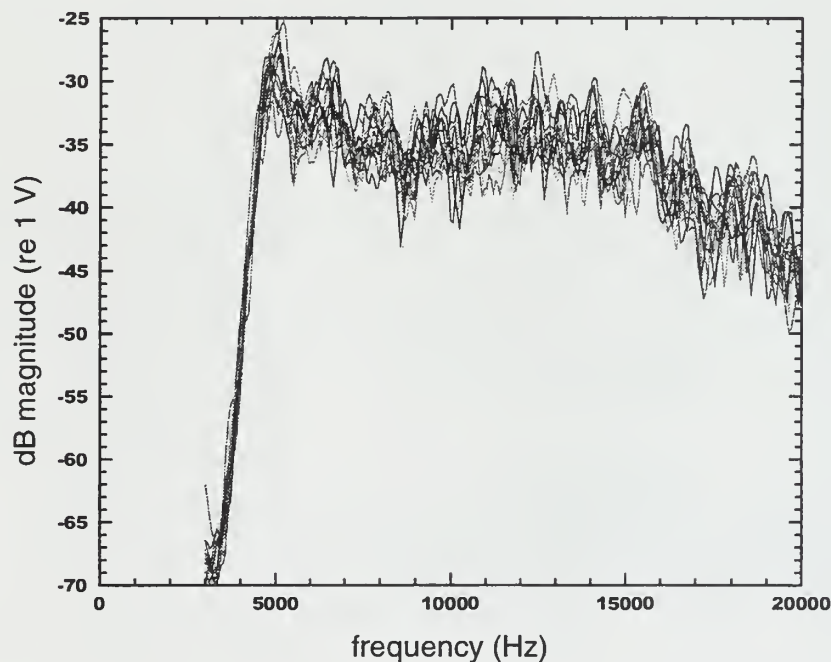
Figure 3.4. Acoustic field intensity measurements for horizontal locations 34-44-54 cm measured left/right and vertical(high/low/center) for 5 kHz to 20 kHz. The spectrum is essential flat from 5 kHz to 15 kHz, rolling off 20 dB from 15 to 20 kHz.

B.   OPTICAL BENCH WITH STEP MOTOR

The step motor was mounted on a small aluminum optical bench, Figure 3.5(A).   The three-point leg adjustments of the bench compensated for the tank curvature allowing for leveling of the step motor and attached plate. The step

motor is a Vexta PH266-02-A29, 2-phase, 1.8 degree/step, 12 V dc motor which provides accurate repeatable plate separation. The number of steps (1 to 255 steps) and direction (up or down) are controlled through a microchip controller. Attached to a machined screw with 20 threads/inch, the step motor mount yields a displacement ranging from 6.35 µm for one step (1.8 degrees) to 1.27 mm for 200 steps (360 degrees).
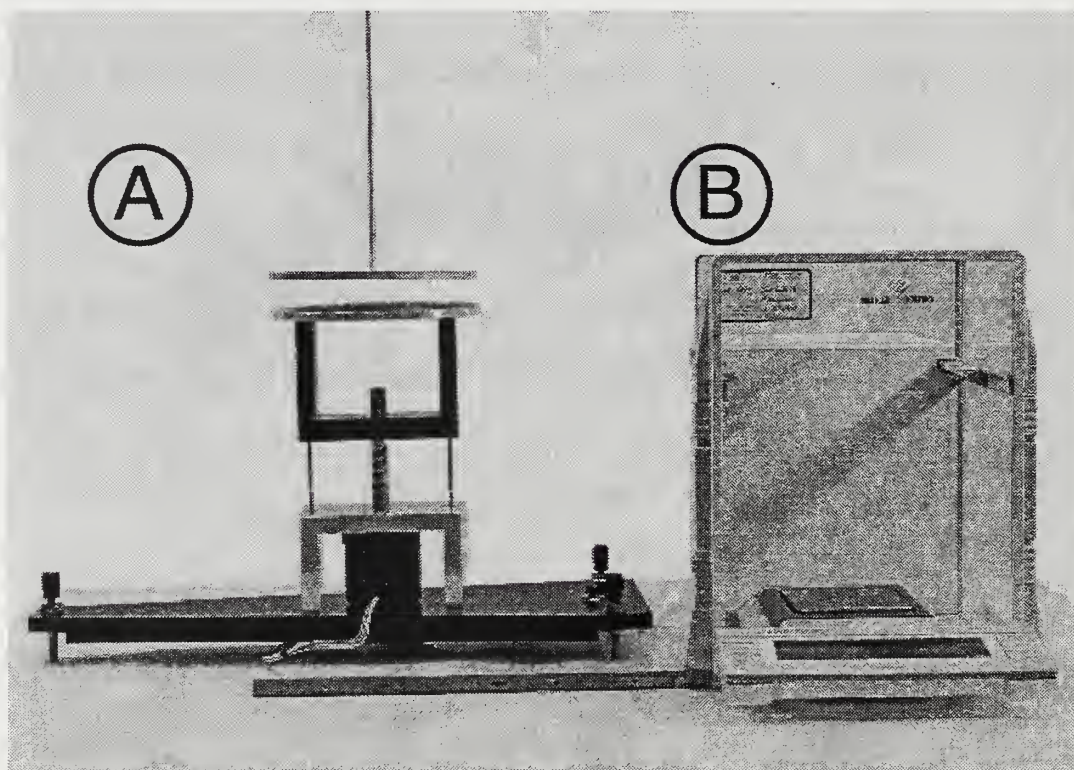
Figure 3.5. (A) Optical bench with microchip-controlled step motor providing precise plate separation. The bottom plate is aluminum [15cm diameter, 6.35mm (1/4 inch) thick] and the top plate is vacuum aluminized PVC [15cm diameter, 5.57mm (7/32 inch) thick]. **(B)** The top plate hangs beneath the Mettler-Toledo AT261 AT analytical balance for force measurement (below-balance weighing).

The step motor displacement was verified through the range of the machined screw using a linear variable differential transformer (LVDT). Figure 3.6 shows the static calibration curve for the LVDT. The primary coil source of

the LVDT was a SR DS345 function generator. The secondary coil output was connected to a SR850 DSP lock-in amplifier, and displacement measurements were done with a micrometer.
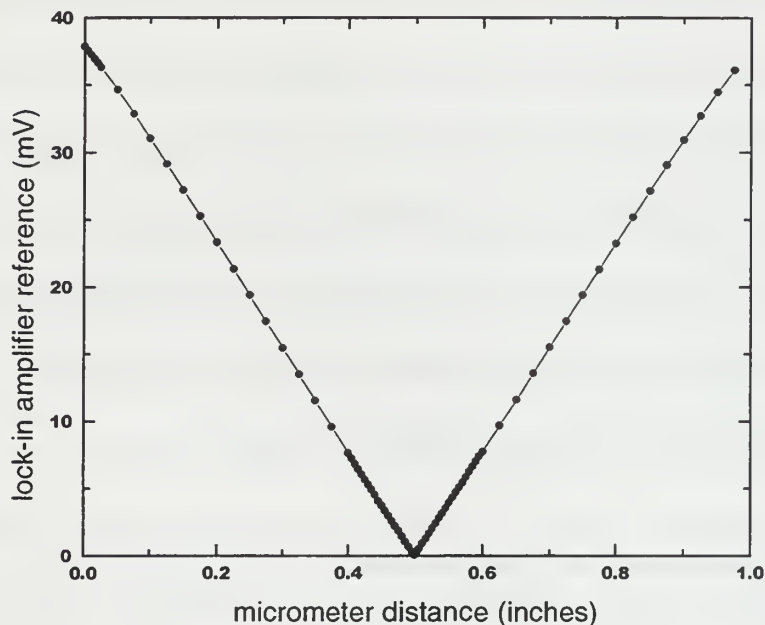
Figure 3.6. LVDT static calibration showing linear and non-linear regions. The slope of the curve in the linear regions provides a calibration factor of 78.04±0.6% mV/in. When this calibration factor is used in conjunction with mV/step measurements for the step motor mount it yields a value of 1.27 mm or 20 threads per inch.

Two 15 cm diameter plates were used for the acoustic Casimir force measurement. The bottom plate was aluminum (6.35 mm or 1/4 inch thick), which was attached firmly on top of the step motor mount. The top plate was vacuum aluminized PVC (5.57 mm or 7/32 inch thick), which was hung beneath the analytical balance. Both plates were grounded to a common ground to eliminate electrostatic effects.

C.   ANALYTICAL BALANCE

For 20 cm by 20 cm plates, at a separation less than 0.3 cm in a 5 kHz to 15 kHz frequency range the force acting on two plates due to acoustic radiation pressure is calculated to be approximately 0.1 mN at 120 dB (re 20uPa), which corresponds to a weight of 10.2 mg. To meet such high resolution weight measurements, we used a Mettler-Toledo AT261 Delta Range AT analytical balance, Figure 3.5(B), with fully automatic self-calibration (FACT) and ISO 9001 certification. The weight of a 15 cm diameter, ¼" thick PVC plate is roughly 150 g, which is well within the 205 g weighing capability of the AT261. The characteristics of the AT261 are outlined in Table 1.

Model	Weighing Capacity	Readability	Repeatability
AT261 Delta Range	62 g (when tared)	0.01 mg	0.015 mg
	205 g	0.1 mg	0.05 mg

Table 1. Mettler-Toledo AT261 Delta Range analytical balance characteristics.

IV. EXPERIMENTAL RESULTS AND CONCLUSIONS

A. EXPERIMENTAL METHOD

To measure the acoustic Casimir force, the optical bench with step motor was centered in the acoustic chamber 46 cm from the tank access. As indicated by a leveling bubble, the three height adjustment screws were used to level the step motor mount with the bottom plate attached. The top plate was hung from the Mettler-Toledo AT261 analytical balance and the bottom plate was raised beneath it. The plates were visually aligned parallel, and the initial plate spacing was determined with a spark plug gap gauge. The plate separation was verified, within the human eye resolution of 0.03 mm, to be uniform by measurements at two or three different locations between the plates. A Larson Davis 2530 microphone was positioned within a centimeter of the top plate to provide spectrum intensity measurements. The acoustic chamber was sealed and the system allowed to stabilize. Once the oscillations of the top plate damped out and the balance reading locked in on the weight of the plate top, which was 168.1653 g, the balance was tared to zero. All force measurements were made relative to this zero. Figure 4.1 gives an internal view of the experimental setup.

The plate separation was controlled remotely through the use of a microchip step motor controller. The controller was set to rotate the step motor 200 steps, 1.8 degrees per step, for a total of one revolution (360 degrees). Each activation of the controller separated the plates by 1.27 mm, moving the bottom plate downwards through a range of 6.3 cm.
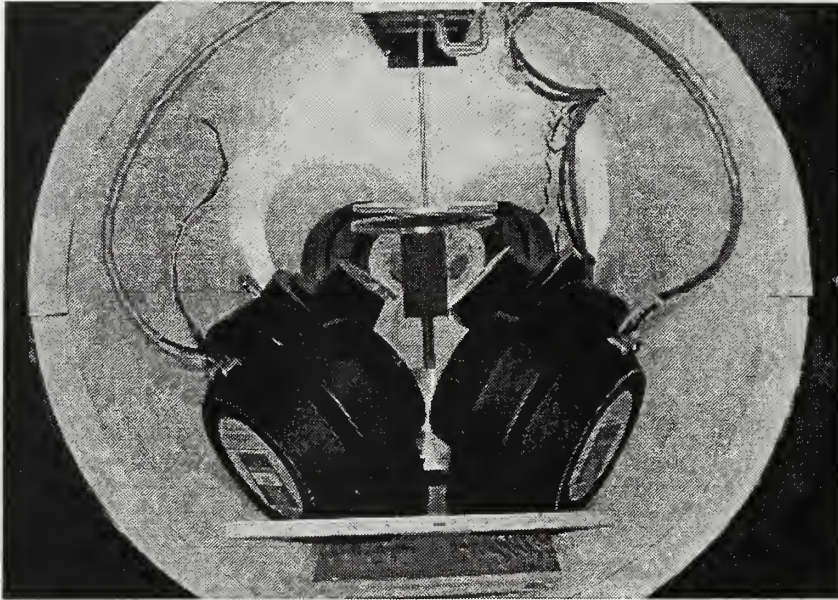
Figure 4.1. Internal view of acoustic Chamber showing equipment arrangement. The step motor mount is 48 cm from the open end.

Force measurements were carried out sequentially. The acoustic field was turned on for each step and the force measurement recorded once the balance readout first locked-in. Simultaneously, the internal microphone measured the sound field intensity which was averaged over 50 measurements using a HP 35670A dynamic signal analyzer. The sound field was then turned off and the reading of the balance was verified to return to zero. The plates were displaced an additional 1.27 mm, and the measurement procedure described above was repeated through the full 6.3 cm range of the step motor mount.

B.   MEASUREMENTS

For the initial experiment, we selected an ideal uniform broadband noise spectrum between 5 and 15 kHz. The lower limit was selected well above the lower modes of the tank in order to excite a noise distribution as homogeneous as possible. The upper limit was selected because the JBL 2445J compression

drivers roll off 20 dB above 15 kHz. To establish a relatively flat 5 - 15 kHz

spectrum, speakers 1 and 2 were driven at 5 - 15.2 kHz and speakers 3 to 6 at

10 - 16 kHz. Figure 4.2 shows the measured noise spectrum of 133 dB (re 10^{-12}

W/m^2), which except for 5 dB variations throughout, is nearly flat within the

spectral range of 4.8 kHz to 16 kHz.
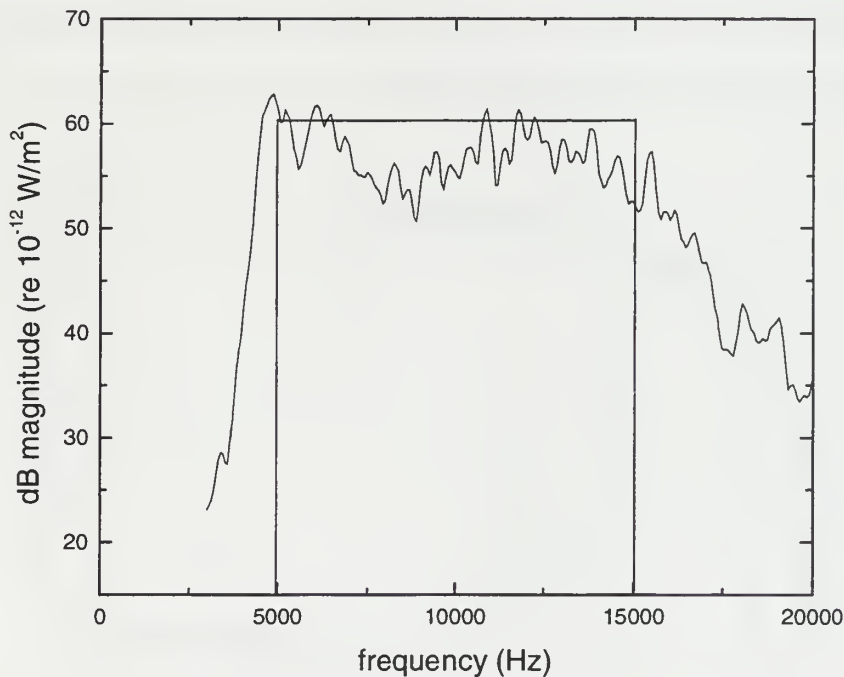
Figure 4.2. Ideal ("brick wall") 5 - 15 kHz spectrum compared to actual 4.8 - 16 kHz relatively flat spectrum showing structure (dip) and an overall 5 dB roll off. The total intensity of the noise corresponds to 133 dB (re 10^{-12} W/m^2).

Using a spark plug gauge, the initial plate separation was measured to be

0.76 mm. As shown in Fig. 4.3, throughout a range of distances less than the

smallest half wavelength (no normal modes between the plates), the measured

force is approximately independent of distance, and agrees with the expected

value for an intensity level of 133 dB (re 10^{-12} W/m^2). When the half wavelength

of the highest frequency fits between the plates (10.63 mm half wavelength for 16 kHz), the force begins to decrease. The force shows the interesting characteristics of a step function at approximately 15 - 20 mm separation and a repulsive force (i.e., negative) from 30 - 40 mm. The results show excellent qualitative agreement and good quantitative agreement between experiment and theory. The theory (Chapter II) has no adjustable parameters. The differences between experiment and theory can be attributed to the structure present in sound spectrum and the slight roll off of 5 dB.

Figure 4.3. Force between two parallel rigid plates as a function of the separation between them. The force is due to the radiation pressure of flat noise between 5 kHz - 15 kHz. The total intensity of the noise is 133 dB (re 10^{-12} W/m^2). The experiment (points) and theory (curve) are in excellent qualitative agreement and good quantitative agreement. The differences are due to the structure of the spectrum of Fig 4.2 and a 5 dB roll off of the spectrum compared to the ideal (5 - 15 kHz) flat spectrum.

Next we selected a frequency band between 7.5 - 15 kHz to investigate what effect a different spectrum would have on the acoustic Casimir force. To achieve a 7.5 - 15 kHz flat spectrum, speakers 1 and 2 were driven at 7.5 - 10.2 kHz and speakers 3 to 6 at 10 - 17 kHz. Figure 4.4 show the measured spectrum of 133.5 dB (re 10^{-12} W/m^2) noise to be nearly flat between 7.4 - 15.3 kHz.
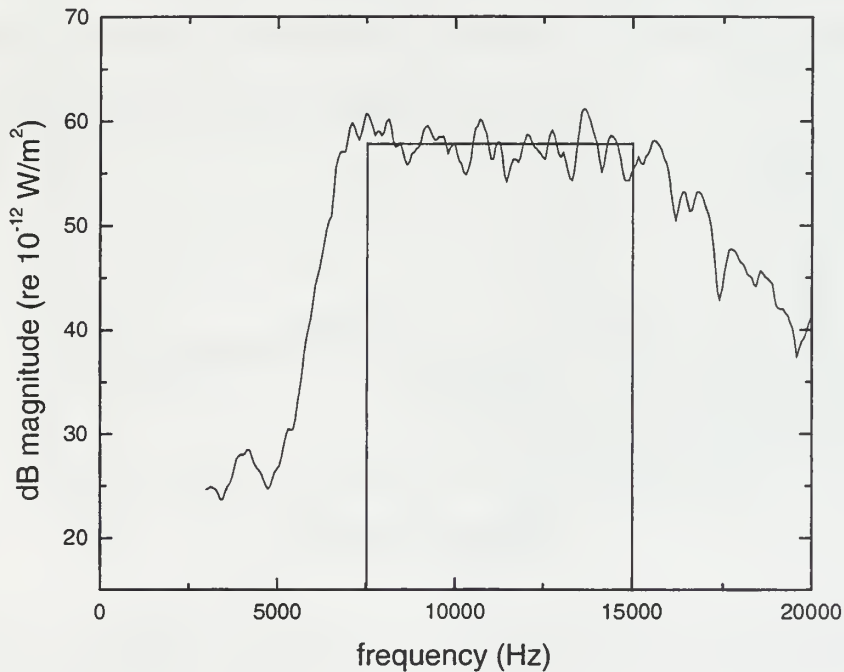
Figure 4.4. Ideal ("brick wall") 7.5 - 15 kHz spectrum compared to actual 7.4 - 15.3 kHz spectrum showing less structure and a flatter spectral shape. The total intensity of the noise corresponds to 133.5 dB (re 10^{-12} W/m^2).

With this spectrum, we set the initial plate separation to 0.96 mm. Figure 4.5 shows again that the force between the plates is independent of distance up to about 11.11 mm, corresponding to the half wavelength of the highest frequency. Note that a repulsive force starts at a smaller distance (20 mm),

covering a larger range (20 - 40 mm) than in the previous case, in agreement

with theory. The results again showed excellent qualitative agreement and better

quantitative agreement than in Figure 4.3. The improved quantitative agreement

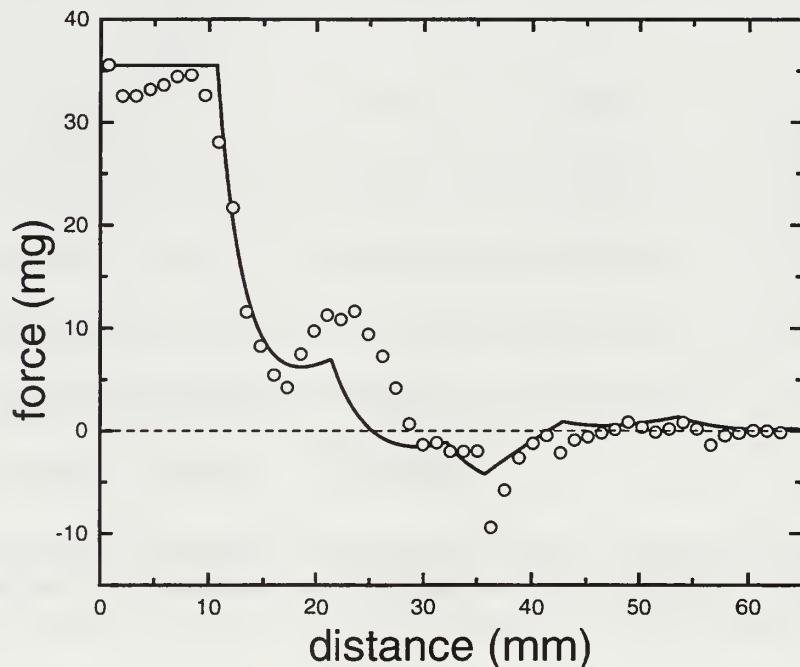is due to the flatter spectrum with less overall structure.
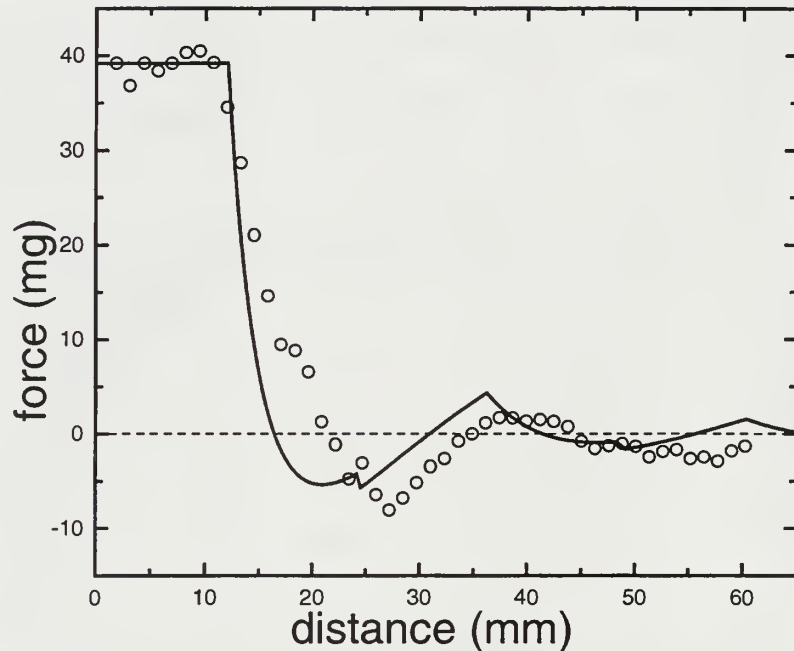
Figure 4.5. Force between two parallel rigid plates as a function of the separation between them. The force is due to the radiation pressure of flat noise between 7.5 kHz - 15 kHz. The total intensity of the noise is 133.5 dB (re 10^{-12} W/m^2). The experiment (points) and theory (curve) are in excellent qualitative agreement. A better quantitative agreement than the one shown in Fig. 4.3 is due to a refined flatter spectrum with less structure.

C. CONCLUSIONS

Casimir (1948) predicted that two closely spaced uncharged conducting

plates would be mutually attractive. M.J. Sparnaay (1958), attempted direct

measurement of the Casimir force in a vacuum achieving measurements of the

28

right shape, but with 100% uncertainty. S. K. Lamoreaux (1997), was the first to

measure the Casimir force, the vacuum stress between two closely spaced

conducting surfaces due to the modification of the zero point fluctuations of the

electromagnetic field, in a 0.6 - 6 µm range. Concurrently, here at the Naval

Postgraduate School, the acoustic Casimir effect was conclusively demonstrated

with the advantage of further experimentation. This successful experiment has

opened up the field of Casimir acoustics as a viable means to investigate and

probe by analogy effects due to the zero point field.   It has taken a half century,

but Casimir's theory has become reality, Figure 4.6.

1997: NPS measures Acoustic
Casimir Analog Effect

1997:S.K. Lamoreaux measures
ZPF Casimir Effect at 0.6-6um

1958: M.J. Sparnaay attempts measurements
(right shape with 100% uncertainty)

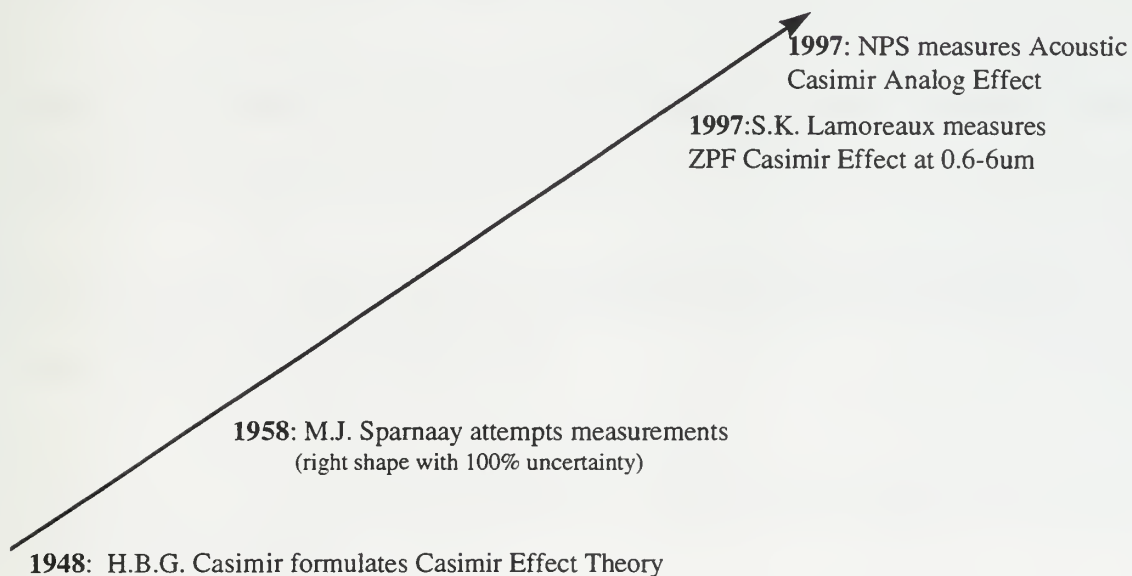**1948**: H.B.G. Casimir formulates Casimir Effect Theory

Figure 4.6. Casimir Effect: Theory to acoustic Casimir effect reality in 50 years.

We can also note that the acoustic Casimir effect can be a potential tool

in noise transduction. Current methods of determining background noise utilize

time averaged microphone or hydrophone measurements. The acoustic Casimir

effect suggests a method of determining the background noise through direct measurement of the force between two plates, or any other cavity. The shape of the force over distance is an instantaneous time average over all frequencies and may provide an alternative to measurements of background noise.

Experimental evidence of attractive and repulsive forces within a finite acoustic bandwidth suggest also new means of acoustic levitation. The force between two objects can be manipulated by changing the distance between the objects and/or varying the spectrum. While the Casimir force is small compared to the force of the Earth's gravity, in a low gravity environment, (i.e., International Space Station), a method of material control through the manipulation of an acoustic spectrum or plate geometry may be possible.

LIST OF REFERENCES

Boyer, T., "Derivation of the Blackbody Radiation without Quantum Assumptions," *Phys. Rev.* **182**, 1374-1383, 1969.

Casimir, H. B. G., "On the Attraction Between Two Perfectly Conducting Plates," *Proc. Kon. Ned. Akad. Wetensch.* **51**, 793-796, 1948.

Casimir, H. B. G., and D. Polder, "The Influence of Retardation on the London-van der Waals Forces," *Phys. Rev.* **73**, 360-372, 1948.

Eberlein, C., "Theory of Quantum Radiation Observed as Sonoluminescence," *Phys. Rev. A* **53**, 2772-2787, 1996.

Haisch, B., A. Rueda, and H. E. Puthoff, "Inertia as a Zero-Point-Field Lorentz Force," *Phys. Rev. A* **49**, 678-694, 1994.

Lamoreaux, S. K., "Demonstration of the Casimir Force in the 0.6 to 6 μm Range," *Phys. Rev. Lett.* **78**, 5-8, 1997.

Lifshitz, E. M., "The Theory of Molecular Forces Between Solids," *Sov. Phys. JETP* **2**, 73-83, 1956.

Sakurai, J. J., *Advanced Quantum Mechanics* (Addison-Wesley, London), Secs. 2-4. and 2-8, 1967.

Schwinger, J., "Casimir Light: The Source," *Proc. Natl. Acad. Sci.* **90**, 2105-2106, 1993.

Schwinger, J., L. DeRaad, and K. A. Milton, "Casimir Effect in Dielectrics," *Ann. Phys.* **115**, 1-23, 1978.

Sparnaay, M. J., "Measurements of Attractive Forces Between Flat Plates," *Physica* **24**, 751-764, 1958.

Susbilla, R. T., "Casimir Acoustics", Master's thesis, Naval Postgraduate School, Monterey, California, 1996.

INITIAL DISTRIBUTION LIST

1.   Defense Technical Information Center...2
   8725 John J. Kingman Rd., STE 0944
   Ft. Belvoir, VA 22060-6218

2.   Dudley Knox Library...2
   Naval Postgraduate School
   411 Dyer Rd.
   Monterey, CA 93943-5101

3.   Professor Hendrik Casimir...1
   De Zegge 17
   5591 TT Heeze
   The Netherlands

4.   Dr. A. Larraza, Code PH/La..2
   Department of Physics
   Naval Postgraduate School
   Monterey, CA 93943-5002

5.   Dr. B. Denardo..2
   National Center for Physical Acoustics
   University of Mississippi
   One Coliseum Drive
   University, MS 38677

6.   Dr. W. B. Colson, Code PH/Cw...1
   Department of Physics
   Naval Postgraduate School
   Monterey, CA 93943-5002

7.   Professor J. Luscombe, Code PH/Lj...1
   Department of Physics
   Naval Postgraduate School
   Monterey, CA 93943-5002

8.   Professor W. Maier, Code PH/Mw...1
   Department of Physics
   Naval Postgraduate School
   Monterey, CA 93943-5002

9.   LT C. D. Holmes..2
   R.D.1 Box 475
   Cobleskill, NY 12043